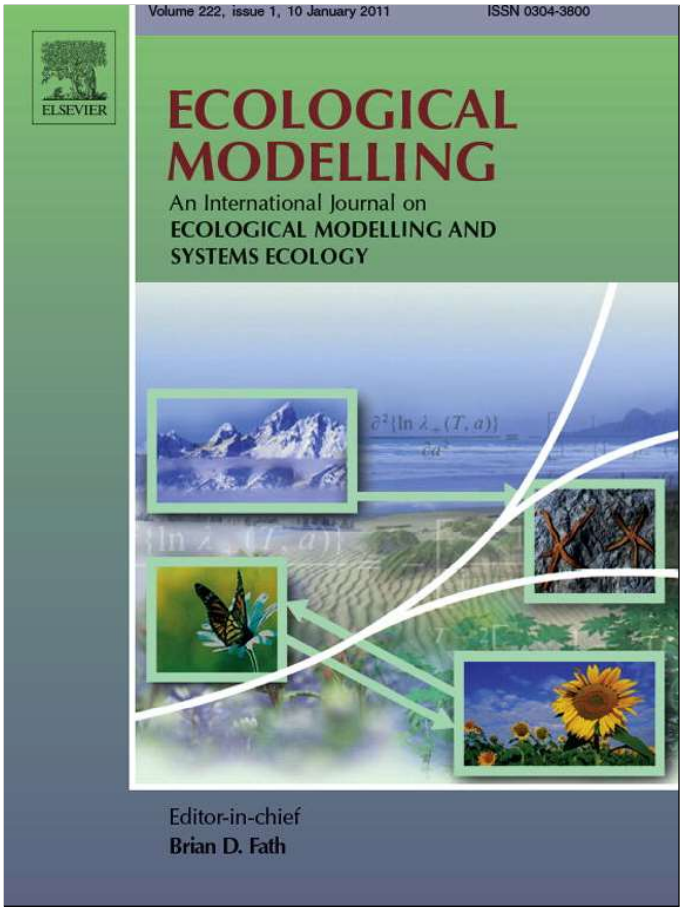

(This is a sample cover image for this issue. The actual cover is not yet available at this time.)

Ecological Modelling 225 (2012) 19–27

Contents lists available at SciVerse ScienceDirect

Ecological Modelling

journal homepage: www.elsevier.com/locate/ecolmodel

Modeling the influence from ocean transport, mixing and grazing on phytoplankton diversity

Mohamed Adjou [a,*], Jørgen Bendtsen [a,b], Katherine Richardson [a]

[a] Center for Macroecology, Evolution and Climate, Department of Biology, University of Copenhagen, Universitetsparken 15, DK-2100 Copenhagen O, Denmark
[b] VitusLab, Symbion Science Park, Fruebjergvej 3, 2100 Copenhagen O, Denmark

ARTICLE INFO

Article history:
Received 7 July 2011
Received in revised form 30 October 2011
Accepted 2 November 2011

Keywords:
Phytoplankton diversity
Exclusion
Co-existence
Competition
Functional groups
Grazing
Phytoplankton transport

ABSTRACT

Phytoplankton diversity, whether defined on the basis of functional groups or on the basis of numbers of individual species, is known to be heterogeneous throughout the global ocean. The factors regulating this diversity are generally poorly understood, although access to limiting nutrients and light is known to influence distributions for certain groups of phytoplankton. Here, we develop a simple box model of biomasses and a limiting nutrient to describe the composition of phytoplankton communities in the euphotic zone. In addition to analyzing the relative importance of nutrient availability in generating and maintaining diversity, we apply the model to quantify the potential role of zooplankton grazing and ocean transport for the coexistence of competing species and phytoplankton diversity. We analyze the sensitivity of phytoplankton biomass distributions to different types of grazing functional responses and show that preferential grazing on abundant species, for example as formulated by the Holling type III grazing function, is a key factor for maintaining species' coexistence. Mixing and large-scale advection are shown to potentially have a significant impact on the distribution of phytoplankton species and, in general, enhance phytoplankton diversity. Based on the model solutions, we argue that ocean transports of phytoplankton cells can have a significant influence on species composition and that even transports at horizontal spatial scales of up to at least 10^2 km and vertical scales of 10^2 m can be expected to be important for sustaining phytoplankton diversity. The model is applied in a multi-species simulation ($n = 200$) and model simulations suggest that global patterns of phytoplankton biodiversity are determined by a few dominating species within each group. This finding is shown to be in accordance with ecological observations.

1. Introduction

Phytoplankton diversity impacts both the structure of marine food webs (e.g. Cushing, 1989) and the ability of the ocean to function as a natural carbon sink (e.g. De La Rocha and Passow, 2007). It is important, therefore, to understand the mechanisms controlling phytoplankton diversity in order to address how environmental change may alter marine ecosystems. The question of what determines phytoplankton diversity has plagued scientists for generations. Most ecological theory – including that relating to the interaction between species – takes as its starting point terrestrial ecosystems and it was on the basis of observations here that the *principle of competitive exclusion* (Gause, 1934; Hardin, 1960) was formulated. This states that two species competing for the same resource cannot coexist and the number of coexisting species cannot exceed the number of limiting resources.

The large number of phytoplankton species observed in the marine environment seems to contradict this principle and this was, subsequently, identified as *the paradox of the plankton* (Hutchinson, 1961). Various mechanisms have since been suggested as being responsible for the coexistence of species and the large phytoplankton diversity. These include (i) stochastic changes in environmental conditions leading to non-equilibrium coexistence (e.g. Deangelis and Waterhouse, 1987; Litchman and Klausmeier, 2001), (ii) oscillations and chaotic fluctuations in species abundances generated by multi-species competition for more than two nutrients (Huisman and Weissing, 1999, 2001), and (iii) selective grazing, as initially proposed by Hutchinson (1961).

The latter mechanism has been investigated in many laboratory and field studies, where it has been shown that zooplankton selectively predate depending on size, "taste", and morphology of the phytoplankton prey (Burns, 1968; Arnold, 1971; Margalef, 1978; Grover, 1989; Naselli-Flores et al., 2007). It has also been argued that selective grazing may, primarily, be due to various specific defense strategies developed during the evolutionary history of phytoplankton (Smetacek, 2001), rather than resulting from direct

* Corresponding author.
E-mail address: MAdjou@bio.ku.dk (M. Adjou).

0304-3800/$ – see front matter © 2011 Elsevier B.V. All rights reserved.
doi:10.1016/j.ecolmodel.2011.11.005

prey-specialization. The argument that selective grazing evolved as a result of specific defense strategies is supported by the observation that global distribution of zooplankton diversity does not appear to show any significant correlation with phytoplankton diversity (Irigoien et al., 2004). If grazing was regulated by specific prey-preferences, we would expect a relationship between zooplankton and phytoplankton diversity.

Local environmental conditions, including nutrient availability, turbulent mixing and stratification are also recognized as being potentially important for phytoplankton community structure as originally formulated in Margalef's *Mandala* (1978). In addition, transport and mixing by ocean currents are potentially important drivers for sustaining phytoplankton diversity because they can directly provide a flux of phytoplankton cells (in various stages of their life cycle) to the euphotic zone. Model simulations have shown that ocean dynamics may play a major role for shaping the global pattern of phytoplankton distributions (Barton et al., 2010) and that meso-scale mixing may be important for phytoplankton communities (d'Ovidio et al., 2010). However, an ecological mechanistic understanding of how physical transport may contribute to phytoplankton diversity is still lacking due to the ephemeral nature of pelagic environmental conditions (i.e. eddies and ocean currents).

At the macroecological scale, a unimodal pattern of phytoplankton diversity as a function of biomass has been shown for the global ocean (Irigoien et al., 2004) suggesting a universal mechanism underlying the diversity of the global phytoplankton communities. This relationship, known also as the "hump-shaped" curve was first identified in macroecological observations of terrestrial plants (Rosenzweig, 1995) and where ecological concepts related to competition for resources were suggested as being its cause (e.g. Abrams, 1995; Waide et al., 1999). In contrast, no rational explanation of this global marine phytoplankton relationship has yet been proposed.

The purpose of the model study presented here was to further our mechanistic understanding of how environmental factors may control large scale phytoplankton community structure. We introduce a new model for phytoplankton community composition based on phytoplankton growth kinetics and mortality and where nutrient input and phytoplankton cell transport to the euphotic zone are explicitly resolved. We then use the model to analyze the sensitivity of the diversity recorded by the model to various relationships between grazing pressure and phytoplankton biomasses and to determine the potential role of physical transports of phytoplankton cells and nutrient input to the surface layer in creating/maintaining diversity. The model results are discussed in light of results from relevant field studies.

2. Methods

2.1. Model description

The model describes phytoplankton species' biomasses as a function of nutrient input to the surface layer, mortality and grazing pressure. In addition, the model considers the transport of phytoplankton cells (continuous inoculation), which can be interpreted both as a direct transport of vegetative phytoplankton cells and as a transport of phytoplankton in other stages (i.e. cysts or resting spores) of their life cycle (Fig. 1).

We choose nitrate, here referred to as "nitrogen", to represent a general nutrient limitation. Other limiting factors such as phosphorous, silicate, light, or micro-nutrients could, correspondingly, be substituted. Biomasses of different species/groups (B_i) are defined in units of nitrogen (μmol N L^{-1}) and they are regulated by the phytoplankton growth rate (μ_i) defined by Monod kinetics

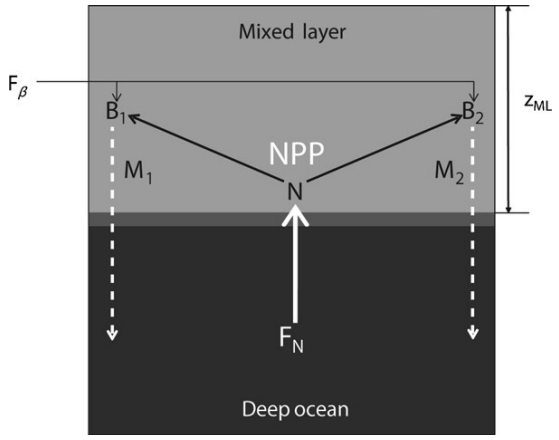

Fig. 1. Schematic representation of the model in a configuration with two phytoplankton species' biomasses (B_1 and B_2), new primary production (NPP), grazing and natural mortalities (M_i), nutrient flux (F_N) and a transport flux of biomasses (F_β).

for phytoplankton growth (Tian, 2006 and references therein) and mortality:

$$\mu_i = \mu_{mi}\frac{N}{N+K_i} \quad (1)$$

where index i represents the biomass of the individual species ($i = 1, n$), N is the nitrogen concentration (μmol L^{-1}), μ_{mi} is the maximum net growth rate (d^{-1}) and K_i is the associated half-saturation constant (Fig. 2a).

Phytoplankton mortality is due to a "natural mortality" (m), including processes such as viral lysis and sinking out of the euphotic zone and a mortality due to grazing (G_i) from higher trophic levels represented by a total biomass of zooplankton grazers (Z). The total phytoplankton mortality (M_i) is then defined as $M_i = G_iZ + mB_i$

We analyze the model sensitivity to three different functional descriptions (types) of grazing (Holling, 1959; Fasham, 1995) and phytoplankton dynamics (Fig. 2b, Table 1). Various parameterizations of zooplankton grazing and phytoplankton production have been applied in previous studies (*see* Gentleman et al., 2003). We further consider the model sensitivity to the HIII parameterization below.

We assume that the zooplankton biomass can be modeled as a function of bulk phytoplankton biomass $\left(\sum_i B_i\right)$:

$$Z = \left(\sum_i B_i\right)^{\alpha} \quad (2)$$

This parameterization is supported by the study Gasol et al. (1997), where a significant log–log correlation between zooplankton and phytoplankton biomasses was observed from several open ocean and coastal locations. This equation is also comparable to the more complicated correlation-function established by Irigoien et al.

Table 1
Grazing mortality parameterizations. Parameter definitions and values are shown in Table 2.

	Grazing function
Constant (HI)	$G_i = \gamma$
Holling type II (HII)	$G_i = g_0\frac{B_i}{k+B_i}$
Holling type III (HIII)	$G_i = \frac{g_0\varepsilon B_i^2}{g_0+\varepsilon B_i^2}$

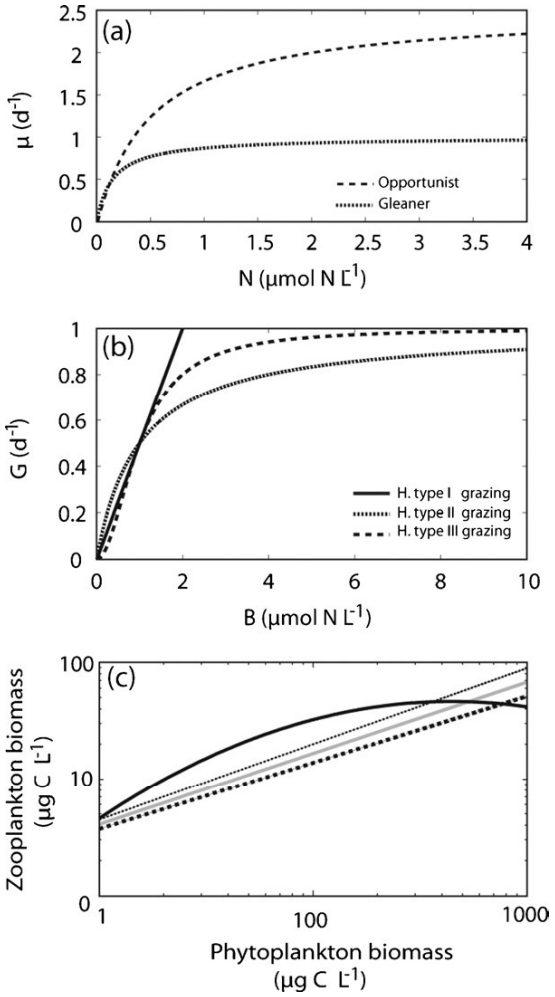

Fig. 2. (a) Growth kinetics of two phytoplankton species (gleaner vs. opportunist) as a function of nutrient concentration (N) where the opportunist's specific growth rate is larger than the gleaner's when $N > 0.08$ μmol L^{-1}. (b) Grazing functional responses (G_i) in three cases: linear grazing (Holling type I), Michaelis–Menten (Holling type II) and sigmoidal (Holling type III). (c) Zooplankton vs. phytoplankton (Z,B) biomass relationship in decimal logarithmic scale from the study of Irigoien et al. (2004) based on observations in the English Channel (full line) and the study of Gasol et al. (1997) shown in three cases: coastal relationship $\alpha = 0.65$ (fine dashed), open ocean $\alpha = 0.57$ (thick dashed line), ocean mean $\alpha = 0.61$ (grey).

(2004) for conditions in the English Channel (Fig. 2c). In our model, we take advantage of this observed relationship between phytoplankton and zooplankton biomasses (Eq. (2)), which reduces the complexity of the model by excluding an explicit zooplankton biomass from the model. We acknowledge, however, that by using this relationship we implicitly assume a specific relationship between the zooplankton growth and mortality terms. For example, it can be shown that using our value of $\alpha = 0.6$ (Table 2), applying a HIII-grazing function and assuming the simple case where the zooplankton mortality scales to a certain power of Z, would imply a zooplankton mortality which scales between the second and the fourth power of the zooplankton biomass for typical ranges of phytoplankton biomasses. Various parameterizations of this mortality term have been applied in previous studies. For example, Edwards and Brindley (1996) applied Z^2 dependence in their explicit modeling of the zooplankton mortality and this formulation is in general accordance with our assumption (Eq. (2)) in a certain range of phytoplankton biomasses.

In addition to net growth, grazing and natural mortality, the phytoplankton species' biomass is also influenced by a contribution from phytoplankton cells transported by ocean currents and mixing ($F_{\beta i}$). The conservation equation for the biomass of a phytoplankton species is, thereby, given by:

$$\frac{dB_i}{dt} = \mu_i B_i - M_i + F_{\beta i} \tag{3}$$

where t is time. The term $F_{\beta i}$ represents the advective and diffusive transport to the mixed layer of phytoplankton species' biomasses (inoculums) by ocean currents and turbulent mixing. $F_{\beta i}$, thus, describes the physical transport of phytoplankton biomass from neighboring waters either in the form of vegetative cells or other life forms. We only consider positive values of $F_{\beta i}$ as negative values, in principle, would correspond to an additional mortality term in Eq. (3). We consider two general cases of the transport term $F_{\beta i}$: in the first case, we assume that all the species have a constant and equal $F_{\beta i} = F_\beta/n$, where F_β is a constant and n is the number of species, and in the second case (referred to as a 'proportional transport') we assume that $F_{\beta i}$ of species i is proportional to its biomass fraction of the total biomass of the mixed layer $F_{\beta i} = F_\beta B_i / \sum_i B_i$.

The total biomass of species inoculums (F_β) was set to relatively low values ranging between 10^{-8} and 10^{-2} μM N L^{-1} d^{-1}. From the two cases with different transport models, we can analyze the potential net effect on diversity from a small transport term both where the rate of transport is the same for all species in the community and where the rate of transport is weighted according to the relative proportion of the biomass each species represents. Transports of biomass and nutrients are treated separately in the model, although these transports may be correlated in the real ocean. Such a correlation can be taken into account in the analysis of the model

Table 2
Model parameters.

Parameter	Value	Parameter description (unit)	Reference
μ_{m1}	1	Maximum B_1 growth rate (d^{-1})	Eppley et al. (1969)[a]
μ_{m2}	2.5	Maximum B_2 growth rate (d^{-1})	Eppley et al. (1969)[a]
K_1	0.15	Half saturation constant of B_1 for nitrate (μmol L^{-1})	Eppley et al. (1969)[a]
K_2	0.50	Half saturation constant of B_2 for nitrate (μmol L^{-1})	Eppley et al. (1969)[a]
NPP	1.53	New Primary Production (mol C m^{-2} yr^{-1})	Martin et al. (1987)
m	0.045	Natural mortality rate (d^{-1})	Fasham et al. (1990)
α	0.61	Exponent relating phytoplankton to zooplankton biomass	Gasol et al. (1997)[b]
γ	0.50	Constant grazing mortality (d^{-1})	Assumed
k	1	Half saturation constant for grazing (μmol N L^{-1})	Fasham (1995)
g_0	1	Maximum grazing rate (d^{-1})	Fasham (1995)
ε	1	Grazing parameter (μmol^{-2} L^3 d^{-1})	Fasham (1995)

[a] Assumed from the ranges of marine phytoplankton species (Eppley et al., 1969).
[b] The slope relationship between zooplankton and phytoplankton logarithmic biomasses was calibrated using carbon mass concentration (mg C m^{-3}), its conversion to the model state variables unit (μmol N L^{-1}) requires a coefficient $\omega = 0.18$.

results by relating the fluxes of $F_{\beta i}$ to the flux of nutrients (F_N), as described below.

The phytoplankton biomasses are defined within the euphotic zone of the upper ocean described by a characteristic mixed layer depth (Z_{ML}). The nutrient concentration is regulated by the phytoplankton uptake and "new production" (*sensu* Dugdale and Goering, 1967) due to the physical transports of nitrogen (F_N) into the mixed layer. F_N equals the net nutrient input into the surface layer and, in steady state; this will equal the new production in the upper layer (Fig. 1). The corresponding conservation equation then becomes:

$$\frac{dN}{dt} = F_N - \sum_i \mu_i B_i \quad (4)$$

In a sensitivity study, we analyze the model solutions for a range of nutrient inputs from 3.2×10^{-4} to 0.2×10^{2} μmol N L^{-1} d^{-1}. In this interval, we define a reference value $F_{N0} \approx 0.02$ μmol N L^{-1} d^{-1} (also shown on a logarithmic scale where $\log_{10}(0.02) = -1.7$) corresponding to estimates of the globally averaged new production of 1.53 mol C m^{-2} yr^{-1} obtained from sediment trap studies (Martin et al., 1987) and assuming a 30 m deep euphotic zone and a C:N Redfield ratio of 6.6 (Redfield et al., 1963). The model equations are integrated numerically to steady state using a fourth order Runge Kutta method.

2.2. Quantification of diversity

The Shannon–Weaver index (H') (Shannon and Weaver, 1949) defined for n species has its maximum value of $\ln(n)$ when all species are represented by equal amounts. Here, we use the species' biomasses, rather than the number of individuals, to calculate H'. This substitution with biomass has also been applied in earlier studies (Barton et al., 2010). Thus, the Shannon–Weaver index is here determined as: $H' = -\sum_i p_i \ln p_i$, where p_i is the biomass of species i divided by the total biomass.

3. Results

3.1. Coexistence and grazing

The role of grazing pressure on phytoplankton diversity was analyzed in a sensitivity study with a no-grazing case and three different grazing parameterizations which frequently have been applied in the literature (Table 1). To elucidate the role of grazing pressure, the model is first analyzed in a simple configuration with only two phytoplankton species (Table 2) and where the influence from transport of phytoplankton biomass is neglected ($F_{\beta i} = 0$). The two species in the model are characterized by their relative growth kinetics, where the opportunist species is characterized by a relatively high growth rate compared to the gleaner's at high nutrient concentrations. In contrast, the gleaner has a relatively high growth rate compared to the opportunist's at low nutrient concentrations (Fig. 2a, Table 2). This relationship between the species is in accordance with earlier studies on nutrient and growth kinetics of phytoplankton species, where the half-saturation constant has been found to be inversely correlated to the specific growth rate (Eppley et al., 1969).

The cases with no-grazing, HI and HII resulted in steady state solutions with only one biomass corresponding to exclusion of one of the species (Fig. 3a–c). Steady state solutions with two biomasses (corresponding to stable coexistence) were only found in the HIII/case (Fig. 3d). The same results are found using the correlation-based equation (Z,B) established by Irigoien et al. (2004) (shown in Fig. 2c), where we find that coexistence is only possible in the case with the Holling type III grazing function.

These results indicate that the strong dependence of grazing on phytoplankton biomass, corresponding to selective grazing as in the Holling type III parameterization, is critical for maintaining a stable coexistence of phytoplankton species. Fig. 3 shows an example with a nutrient input given by $F_N = 10\,F_{N0}$ and initial biomasses at t_0 ($B_{1,2} = 0.01$ μmol N L^{-1}) and nutrient concentration ($N = 0$). Whether it is the opportunist or the gleaner that will be outcompeted depends on initial conditions and F_N.

3.2. Influence of transport and nutrient input on phytoplankton diversity

A sensitivity study was carried out with two phytoplankton species by varying both the nutrient input to the surface layer (F_N) and the direct transport of phytoplankton biomass (F_β) to the surface layer. Model solutions of H' were determined in the four cases with (i) no-grazing, (ii) HI, (iii) HII and (iv) the HIII grazing function (Fig. 4).

In the three cases with no-grazing, HI and HII, respectively, the phytoplankton species can only coexist (corresponding to a high H') when the transport becomes large enough to overcome the mortality rate (Fig. 4a). In the case with HIII, the H' is seen to increase when the nutrient input (F_N) increases to intermediate levels, whereas a

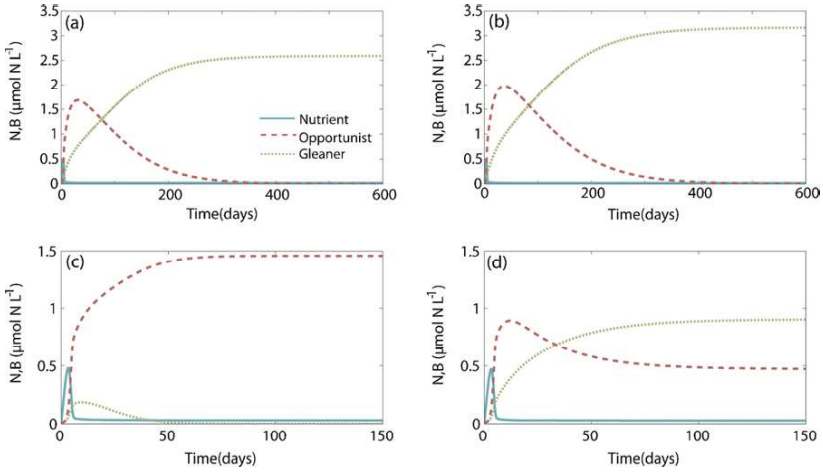

Fig. 3. Exclusion and stable coexistence vs. grazing functional responses. Transient solutions of gleaner biomass, opportunist biomass and nutrient concentration in four cases: no grazing case (a) and three grazing functional responses: (b) HI, (c) HII and (d) HIII. Model solutions are obtained with $F_N = 10\,F_{N0}$ and $F_\beta = 0$ μmol N L^{-1} d^{-1} and initial conditions given by $B_{1,2} = 0.01$ μmol N L^{-1} and $N = 0$ μmol L^{-1}.

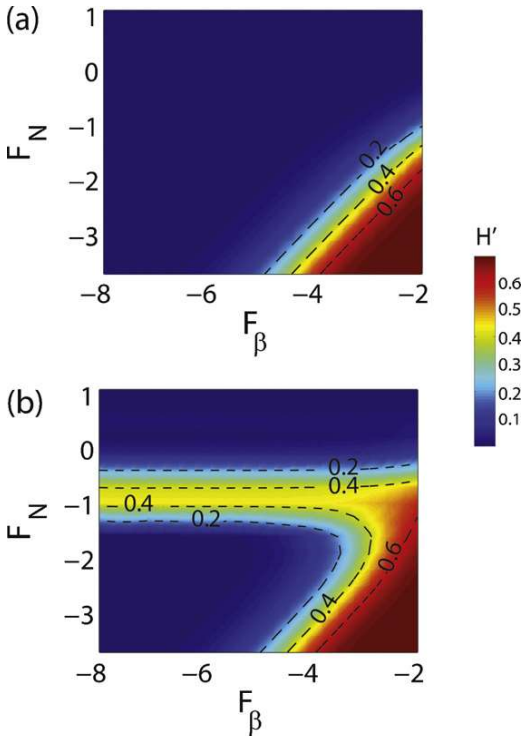

Fig. 4. Shannon–Weaver index (H') for different values of the nutrient flux (F_N) and transport flux (F_β): (a) solutions for no grazing case, HI and HII grazing functional responses and (b) a solution for HIII grazing functional response. Initial conditions for all solutions are: $B_{1,2} = 0\ \mu\text{mol N L}^{-1}$ and $N = 0\ \mu\text{mol L}^{-1}$. F_N and F_β are shown in units of $\log_{10}(\mu\text{mol N L}^{-1}\ \text{d}^{-1})$.

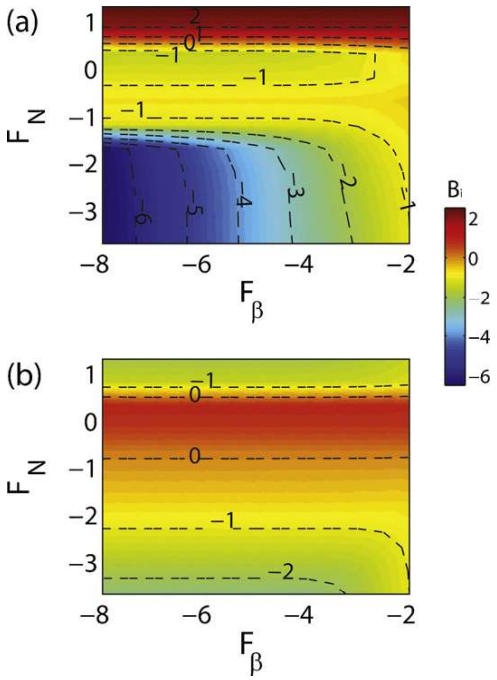

Fig. 5. Biomasses of the opportunist (a) and the gleaner species (b) at steady state for different values of the nutrient flux (F_N) transport flux (F_β, where $F_{\beta i} = F\beta/2$). Solutions are shown for the HIII grazing functional response. Initial conditions for all solutions are given by $B_{1,2} = 0\ \mu\text{mol N L}^{-1}$ and $N = 0\ \mu\text{mol L}^{-1}$. F_N and F_β are shown in units of $\log_{10}(\mu\text{mol N L}^{-1}\ \text{d}^{-1})$. Biomasses ($B_i$) are given is in units of $\log_{10}(\mu\text{mol N L}^{-1})$.

further increase toward very high nutrient input fluxes is seen to reduce the diversity significantly (Fig. 4b).

The analysis of the steady state concentration of the biomasses of the two species reveals that at low F_N, the gleaner dominates, while at high F_N, the opportunist species becomes dominant (Fig. 5). The irregular increase of the biomass of the opportunist (Fig. 5a) with the increase of the nutrient input is due to the non-linearity of the system (i.e. related to the HIII grazing function). Furthermore, for low nutrient inputs ($F_N < F_{N0}$), the opportunist species shows a gradual increase in biomass when the contribution from transport increases (Fig. 5a). The gleaner abundance is, on the other hand, less sensitive to changes in the transport of biomass (Fig. 5b). At relatively high nutrient input levels, there is no significant influence from the transport term on the biomasses of the opportunist and the gleaner (Fig. 5a and b) and, consequently, on the system diversity.

We analyzed the role of grazing in promoting coexistence by increasing the strength of the HIII-function, i.e. by multiplying the grazing term by a constant in the range 1–5 (Fig. 6). Increasing the grazing pressure results in an increase of the Shannon index and also allows for coexistence over a wider interval of nutrient inputs. Analysis of the different forms of the $F_{\beta i}$ parameterizations yielded results that were qualitatively identical.

3.3. Diversity in multi-species simulations

The model result from the two-species simulations showed a modulated structure of relative abundance between the gleaner and the opportunist in different configurations of nutrient input and transport assuming a HIII grazing functional response. To explore this feature in a more realistic multi-species case, we extended the model to include 200 phytoplankton species (Eqs. (3) and (4), $n = 200$). Phytoplankton species were grouped into five functional groups (cyanobacteria, coccolithophorids, diatoms, dinoflagellates and chlorophytes) where all species are competing for the same limiting resource (nitrogen). The growth kinetic parameters for each species were chosen randomly from literature derived intervals characterizing each functional group (Table 3).

The parameterization of the grazing function had to be modified when the number of species is large because the grazing rate becomes unrealistically small for "outcompeted" species when the parameterization is applied at the individual species level (cf. Fig. 2). Therefore, we apply the group bulk-biomass, B_G, of each functional group ($B_G = \sum_i B_{i,G}$) in the calculation of the mortality due to grazing for each species from the same group rather than B_i (Table 1).

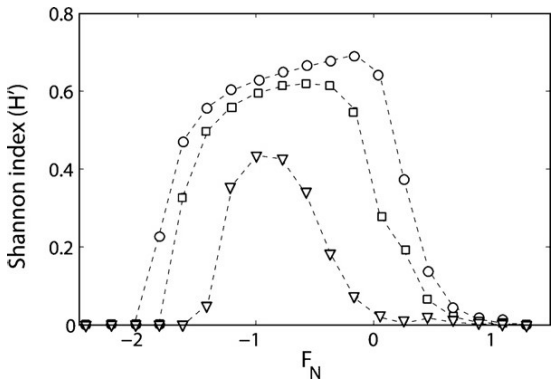

Fig. 6. Diversity (H') of a model solution with 200 species, for different strength of the grazing pressures (triangles shows the reference case and squares and circles show 3 and 5 times higher grazing, respectively) as a function of F_N in units of $\log_{10}(\mu\text{mol N L}^{-1}\ \text{d}^{-1})$. $F_\beta = 10^{-8.3}\ \mu\text{mol N L}^{-1}\ \text{d}^{-1}$.

Table 3
Functional phytoplankton groups and growth parameters.[a]

	Cyanobacteria	Coccolithophorids	Diatoms	Dinoflagellates (autotrophs)	Chlorophycae
K_i (μmol L^{-1})	[0.1–0.25]	[0.25–0.4]	[0.4–0.8]	[1–1.4]	[0.8–1]
μ_{maxi} (d^{-1})	[0.7–0.9]	[1–1.5]	[1–2.5]	[0.2–1.3]	[1–1.7]

[a] Predefined intervals of half-saturation constants and growth rates arbitrarily chosen from the literature (Eppley et al., 1969; Litchman et al., 2007; Dutkiewicz et al., 2009).

This implies that we assume that the grazing rate is similar on all species of the same functional group. Similar grazing parameterizations have been applied in phytoplankton studies where the grazing rate of each functional group is scaled by the total biomass (Lima and Doney, 2004).

The distribution of the Shannon–Weaver index (Fig. 7) shows a comparable behavior of diversity in the 200 species system as to that for the two species system where, in general, a low diversity ($H' < 0.5$) is observed at very low and high nutrient inputs (F_N) compared to the intermediate F_N ($H' = \sim 1.5$). Interestingly, the transition from low to high diversity in the 200 species system is seen in the interval of F_N between 10^{-2} and 10^{-1} μmol N L^{-1} d^{-1}, corresponding to the reference value (F_{N0}) representing the global averaged new production. When the contribution from transport of biomass becomes very high, the diversity increases correspondingly ($H' > 3$). We analyzed the effect from the two transport parameterizations (constant and proportional to biomass fraction) and found no qualitatively difference of the diversity distribution (data not shown).

3.4. Phytoplankton community structure in relation to nutrient inputs and transport

The hump-shaped dependence relating diversity and phytoplankton biomass can be explained by an increasing degree of exclusion at very low or very high nutrient inputs dominated by gleaners (i.e. cyanobacteria) or opportunists (i.e. diatoms), respectively. Fig. 8 shows the abundances of 200 species in 8 cases with different combinations of F_N and F_β at the reference grazing case. The predominant species (>90% of the biomass) at low values of F_N are represented by gleaner species (cyanobacteria) (Fig. 8g and h). The other species' (relative opportunists) fractions, at low nutrient input levels increase when the transport of biomass increases (Fig. 8i). At intermediate nutrient input levels (Fig. 8d–f), the model shows clear coexistence of some phytoplankton species from the same or different functional groups. At high nutrient input regimes (Fig. 8a–c), the predominance of one or two diatom species representing >90% of the bulk phytoplankton biomass leads to a significant decrease in the diversity (Fig. 8b).

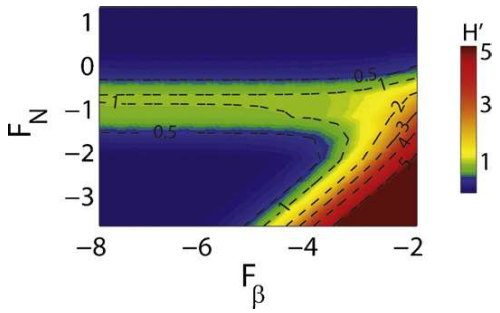

Fig. 7. Steady state solution of the Shannon–Weaver index in a case with 200 different phytoplankton species representing five marine phytoplankton functional groups for different values of the nutrient flux (F_N), transport flux (F_β). F_N and F_β are shown in units of $\log_{10}$(μmol N L^{-1} d^{-1}).

4. Discussion

Studies on phytoplankton diversity focus very often on nutrient availability ('*bottom up processes*') and competition between species for limiting nutrients. This has been the case since the early diversity studies (e.g. Tilman, 1977; Mickelson et al., 1979; Tilman et al., 1982). '*Top down processes*' (e.g. mortality due to grazing), are less understood processes and these have seldom been considered to be important in establishing phytoplankton diversity. This is interesting given the importance of top down processes in determining phytoplankton community structure (e.g. Strom, 2008).

The phytoplankton biodiversity model presented here suggests that selective grazing, nutrient availability and hydrographic features (transport and mixing) all may contribute to establishing and maintaining phytoplankton community diversity. The model describes the conditions within the surface layer as regulated by fluxes of nutrients and small inoculums of species from surrounding water, whereas feedbacks from the surroundings due to, for example, dilution effects are not explicitly included here. The latter assumption is based on the fact that, in general, grazing pressure represents, by far, the main phytoplankton mortality factor (Strom, 2008; Calbet and Landry, 2004). We tested different grazing functional responses where the predator (zooplankton) biomass was estimated from correlative empirical field-relationships based on the prey (phytoplankton) biomass (Gasol et al., 1997; Irigoien et al., 2004) with the aim of reducing the number of free parameters.

The model considers the mean conditions of the surface layer and, therefore, we do not include temporally variable processes that also may influence phytoplankton succession and diversity (Grover, 1990; Huisman and Weissing, 1999, 2001). Phytoplankton diversity in nature is probably also regulated by an interplay between different limiting nutrients, differences in light affinity and other abiotic factors. However, by only considering one limiting nutrient, our model analysis indicates that several limiting nutrients are not a prerequisite for establishing phytoplankton diversity—a high diversity can be sustained by transport mechanisms alone or a high nutrient input to the system.

4.1. Sensitivity of coexistence to functional grazing response

The functional description of the grazing pressure was found to be critical in leading to a stable coexistence of species over a large part of the solution space spanned by F_N and F_β. The HIII grazing function, formulated in accordance with empirical relationships obtained from the marine environment (Fasham, 1995), had a major role in controlling the population abundance by exercising a selective pressure with low grazing rates at low phytoplankton abundance and vice versa.

In the literature, an extensive list of functions is found to describe zooplankton grazing behavior based on theoretical or empirical assumptions (Gentleman et al., 2003). Our study shows that the choice of the grazing type is important for the phytoplankton diversity; HI and HII grazing functions lead to exclusion, whereas HIII promoted coexistence and resulted in higher diversity. The choice of an HIII functional response is supported by laboratory experiments (e.g. Kiorboe et al., 1996; Saage et al., 2009). However, the HIII is not universally accepted as a correct representation

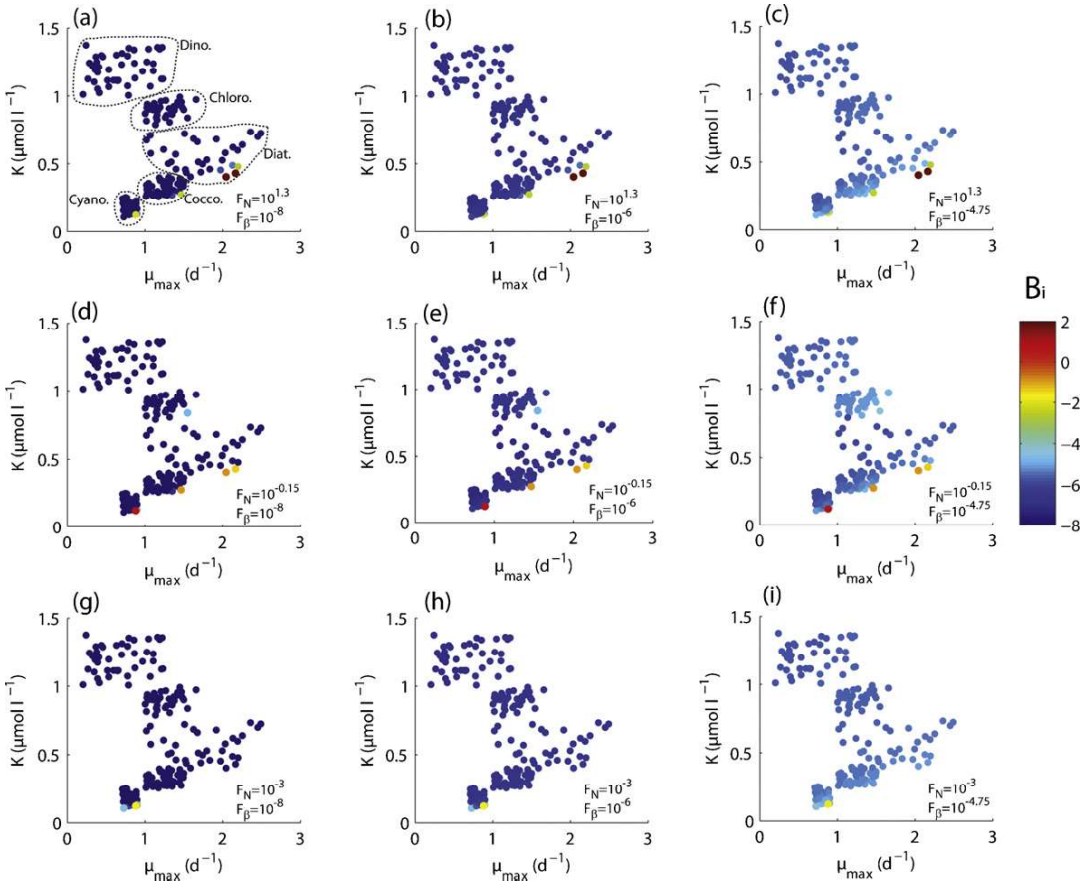

Fig. 8. Model solutions of biomasses in the phytoplankton community. The community is represented by 200 different species chosen randomly from five major phytoplankton functional groups. Species' biomasses are shown in 9 different cases with different nutrient flux (F_N) and transport flux (F_β) indicated in each diagram. Fluxes are in units of [µmol N L^{-1} d^{-1}]. Biomasses (B_i) are given in units of $\log_{10}$(µmol N L^{-1}).

of grazing and, the HII, for example, was found to better describe the grazing behavior of Daphnia (Murdoch et al., 1998). This was addressed by Morozov (2010) who argued that theoretical considerations and field evidence support the HIII functional response. The HIII describes a grazing function stipulating more amortized grazing at low abundances of phytoplankton species. This low grazing pressure behavior at low phytoplankton biomasses could reflects efficient phytoplankton survival strategies in accordance with the defense theories proposed by Smetacek (2001).

4.2. Shannon–Weaver index related to functional groups and grazing pressure

Outside the transport-ranges influencing the diversity ($F_\beta < 10^{-4}$ µmol N L^{-1}), the maximum H' of about 1.5 found in the multi-species simulations is in striking accordance with analyses of the H' found in a global study of phytoplankton diversity (Irigoien et al., 2004) which covered a similar range of phytoplankton biomasses (Fig. 9a and b). If the biomasses were more equally distributed among the 200 species in the model, the corresponding H' would be expected to be significantly higher (with a maximum of 5.3). The relatively low value of about 1.5 found here is close to the value which would be expected if H' mainly was determined by a single dominating species in each functional group (maximum value given by ln(5) = 1.6). This correspondence with the diversity index found in the real ocean suggests that the reported H' indices mainly reflect the number of functional groups or are a consequence of a systematic bias during the counting of the number of cells of each species.

4.3. Diversity from oligotrophic to eutrophic regimes: a universal macroecological signal?

In spite of the fact that the model only operates with one nutrient, the results indicate that phytoplankton diversity, in general, exhibits a unimodal dependence on phytoplankton biomass (Fig. 9). The diversity is found to be relatively low in oligotrophic and hypertrophic regimes and relatively high in mesotrophic to eutrophic regimes. The increase of the grazing intensity, either by increasing zooplankton biomass or grazing activity (i.e. through a Q_{10} temperature effect: Hirst and Bunker, 2003), is shown by the model to enhance diversity.

This finding agrees well with the relationship that emerged from an analysis of global observations of phytoplankton diversity (Irigoien et al., 2004), as well as with the productivity–diversity relationships found in macroecological studies of terrestrial vegetation (Rosenzweig, 1995). That phytoplankton diversity may decline in very nutrient rich regimes may be of interest in relation to coastal eutrophication due to anthropogenic activity. Previously, many eutrophication studies have focused on changes in total primary production or the abundances of different (often harmful) algal species in response to changes in nutrient availability. This

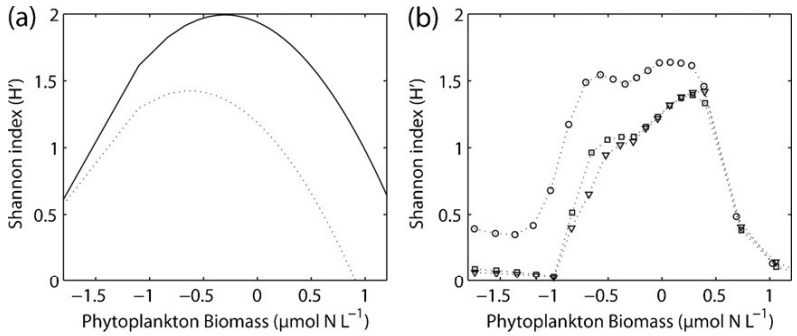

Fig. 9. Unimodal pattern of phytoplankton diversity as a function of phytoplankton biomass. (a) Global distribution of diversity, at high (full line) and low (dashed line) zooplankton biomass obtained from a study of global data (Irigoien et al., 2004). (b) This study: model solution with 200 phytoplankton species ($F_\beta = 10^{-8}$ μmol N L^{-1} d^{-1}) under different grazing pressures (triangles show the reference value and squares and circles show 3 and 5 times higher grazing, respectively).

study suggests that eutrophication may also impact phytoplankton diversity which, in turn, may influence food webs and carbon cycling in the ecosystem.

4.4. Sensitivity of diversity to ocean transports

Typical length scales over which physical transport in the real ocean may become significant for maintaining phytoplankton diversity can be determined from a scale analysis. The transport of phytoplankton cells, described by the term $F_{\beta i}$, can be related to the physical advection and turbulent diffusion of cells:

$$F_{\beta i} = k_\nu = \frac{\partial^2 B_i}{\partial z^2} - u\frac{\partial B_i}{\partial x} \quad (5)$$

where x and z are the horizontal and vertical coordinates, respectively. The vertical turbulent mixing coefficient is described by the diffusion coefficient k_ν and u is the horizontal ocean current velocity (horizontal mixing and vertical advection have been disregarded for simplicity in the analysis below, but corresponding estimates can be made for these transport processes as well). Assuming a typical velocity scale for ocean surface currents of 10 km d^{-1} (∼0.1 m s^{-1}) and a typical value of phytoplankton biomass of 0.01 μmol N L^{-1} implies that the advection term in Eq. (5) becomes of the order of 0.1 μmol N L^{-1} km d^{-1}/λ, where λ is the length scale over which the biomass changes its concentration. According to Fig. 7, the transport starts to have a significant influence on diversity at low nutrient input levels when F_β reaches a value of about 10^{-4} μmol N L^{-1} d^{-1}, corresponding to typical length scale of λ of up to 10^3 km. A biomass transport of 10^{-4} μmol N L^{-1} d^{-1} corresponds to about 1 phytoplankton cell L^{-1} d^{-1}, assuming a typical phytoplankton nitrogen concentration of about 10^{-10} mol N cell^{-1} (Menden-Deuer and Lessard, 2000).

Thus, the scale analysis suggests that a transport of 1 cell over 10^3 km could have a significant influence on the diversity. This demonstrates the potential significance of ocean transport for sustaining diversity. Even a very small transport, representing a transport of phytoplankton cells from a location with a typical biomass to a location with very low concentrations can enhance diversity significantly over long distances. Other factors (i.e. the sinking and grazing mortality of phytoplankton cells) would, of course, limit the transport of phytoplankton cells. A sinking rate of about 10 m d^{-1} would, for example, reduce the length scale to 10–100 km. The model solutions suggest, however, that even with the influence from the sinking of cells, the transport by ocean currents potentially can enhance phytoplankton diversity on length scales of about 10–100 km. This finding agrees well with global model studies (Barton et al., 2010; d'Ovidio et al., 2010; Peterson et al., 2011). In regions with strong current systems, such as western boundary currents with typical ocean currents of 1 m s^{-1}, the potential for transport by ocean currents to influence phytoplankton diversity would increase accordingly.

A similar analysis can be made with respect to the influence from vertical mixing on the input of phytoplankton cells to the surface layer: assuming a typical vertical diffusivity coefficient in the surface layer of 10^{-3} to 10^{-4} m^2 s^{-1} and a similar distribution of biomasses as considered above would result in a vertical length scale of about 100 m. This vertical scale is comparable to the depth of the mixed layer and it shows, for example, that even deep phytoplankton biomasses associated with a subsurface chlorophyll maximum are able to contribute to diversity of phytoplankton at the surface. The above considerations could be extended to cover more robust life stages of phytoplankton (i.e. resting spores or cysts) which can survive during long periods. Thus, even if their typical concentration is very low, they could influence phytoplankton community structure over large distances/depths.

In term of biological observations, the model suggests that gleaners are less influenced by transport at low nutrient input levels than opportunists. This agrees well with field observations. The predominance and the success of gleaners (e.g. cyanobacteria) compared to opportunists (e.g. diatoms) in the tropical oceanic area surrounded by the tropical gyre (Alvain et al., 2005) can potentially be explained by the low nutrient levels there (downwelling) and the diazotrophic ability of cyanobacteria (Montoya et al., 2004). Longhurst (1998) made an analogy between the relatively high biodiversity in ecotones (Odum, 1971), transition zones between two terrestrial ecosystems associated with a high environmental gradient, and the marine areas he compared. Accordingly, Longhurst (1998) argued that there are three major areas that are well distinguished from one another due to physical discontinuities: the continental shelves (neritic areas), meso–scale eddies in the open ocean (pelagic areas), and the most important and the largest: the frontal system areas associated with major water masses or currents. The relatively high observed (Longhurst, 1998) and simulated (Barton et al., 2010; d'Ovidio et al., 2010) diversities in these dynamic areas are in accordance with our model results which predict that transport by ocean currents and eddies would tend to increase diversity.

5. Conclusion

A simple new mechanistic model of phytoplankton diversity in the euphotic zone has been developed and analyzed. The model shows that Holling type III grazing and the grazing intensity are critical for maintaining stable solutions of phytoplankton coexistence between different species, while competition for resources (nutrient availability) mainly controls the community structure.

The model simulates a unimodal relationship between phytoplankton biomass and diversity, where intermediate nutrient levels are associated with relatively high diversity and low and high nutrient levels (biomasses) are associated with relatively low diversity in general accordance with observed global phytoplankton distributions. The model simulates the significance of ocean transports from currents and turbulent mixing and the model results show that physical transport can have a significant impact on phytoplankton diversity over relatively large spatial scales. Our model results suggest that ocean currents could increase diversity significantly on horizontal length scales of up to 100–1000 km and on vertical length scales of about 100 m. Accordingly, physical transports could influence the global distribution of phytoplankton diversity significantly.

Acknowledgement

We acknowledge the Danish National Research Foundation for support to the Center for Macroecology, Evolution and Climate, University of Copenhagen.

References

Abrams, P.A., 1995. Monotonic or unimodal diversity productivity gradients—what does competition theory predict. Ecology 76, 2019–2027.
Alvain, S., Moulin, C., Dandonneau, Y., Breon, F.M., 2005. Remote sensing of phytoplankton groups in case 1 waters from global SeaWiFS imagery. Deep Sea Research Part I-Oceanographic Research Papers 52, 1989–2004.
Arnold, D.E., 1971. Ingestion, assimilation survival, and reproduction by Daphnia-Pulex Fed 7 Species of Blue-Green-Algae. Limnology and Oceanography 16, 906.
Barton, A.D., Dutkiewicz, S., Flierl, G., Bragg, J., Follows, M.J., 2010. Patterns of diversity in marine phytoplankton. Science 327, 1509–1511.
Burns, C.W., 1968. Relationship between body size of filter-feeding cladocera and maximum size of particle ingested. Limnology and Oceanography 13, 675.
Calbet, A., Landry, M.R., 2004. Phytoplankton growth, microzooplankton grazing, and carbon cycling in marine systems. Limnology and Oceanography 49, 51–57.
Cushing, D.H., 1989. A difference in structure between ecosystems in strongly stratified waters and in those that are only weakly stratified. Journal of Plankton Research 11, 1–13.
d'Ovidio, F., De Montec, S., Alvain, S., Dandonneau, Y., Levy, M., 2010. Fluid dynamical niches of phytoplankton types. Proceedings of the National Academy of Sciences of the United States of America 107, 18366–18370.
De La Rocha, C.L., Passow, U., 2007. Factors influencing the sinking of POC and the efficiency of the biological carbon pump. Deep Sea Research Part II-Topical Studies in Oceanography 54, 639–658.
Deangelis, D.L., Waterhouse, J.C., 1987. Equilibrium and nonequilibrium concepts in ecological models. Ecological Monographs 57, 1–21.
Dugdale, R.C., Goering, J.J., 1967. Uptake of new and regenerated forms of nitrogen in primary productivity. Limnology and Oceanography 12, 196-&.
Dutkiewicz, S., Follows, M.J., Bragg, J.G., 2009. Modeling the coupling of ocean ecology and biogeochemistry. Global Biogeochemical Cycles 23.
Edwards, A.M., Brindley, J., 1996. Oscillatory behaviour in a three-component plankton population model. Dynamic Stability of Systems 11, 347–370.
Eppley, R.W., Rogers, J.N., Mccarthy, J.J., 1969. Half-saturation constants for uptake of nitrate and ammonium by marine phytoplankton. Limnology and Oceanography 14, 912.
Fasham, M.J.R, 1995. Variations in the seasonal cycle of biological production in sub-arctic oceans—a model sensitivity analysis. Deep Sea Research Part I-Oceanographic Research Papers 42, 1111–1149.
Fasham, M., Ducklow, H., McKelvie, S., 1990. A nitrogen-based model of plankton dynamics in the oceanic mixed layer. Journal of Marine Research 48 (3), 591–639.
Gasol, J.M., del Giorgio, P.A., Duarte, C.M., 1997. Biomass distribution in marine planktonic communities. Marine Ecology Progress Series 42, 1353–1363.
Gause, G.F., 1934. Experimental analysis of Vito Volterra's mathematical theory of the struggle for existence. Science 79, 16–17.
Gentleman, W., Leising, A., Frost, B., Strom, S., Murray, J., 2003. Ecosystem models with multiple nutritional resources: a critical review of the assumed biological dynamics. Part I. Zooplankton intake. Deep Sea Research II 50, 2847–2875.
Grover, J.P., 1989. Effects of Si–P supply ratio supply variability, and selective grazing in the plankton—an experiment with a natural algal and protistan assemblage. Limnology and Oceanography 34, 349–367.
Grover, J.P., 1990. Resource competition in a variable environment—phytoplankton growing according to Monods model. American Naturalist 136, 771–789.
Hardin, G., 1960. Competitive exclusion principle. Science 131, 1292–1297.
Hirst, A.G., Bunker, A.J., 2003. Growth of marine planktonic copepods: global rates and patterns in relation to chlorophyll a, temperature, and body weight. Limnology and Oceanography 48, 1988–2010.
Holling, C.S., 1959. Some characteristics of simple types of predation and parasitism. Canadian Entomologist 91, 385–398.
Huisman, J., Weissing, F.J., 1999. Biodiversity of plankton by species oscillations and chaos. Nature 402, 407–410.
Huisman, J., Weissing, F.J., 2001. Biological conditions for oscillations and chaos generated by multispecies competition. Ecology 82, 2682–2695.
Hutchinson, G.E., 1961. The paradox of the plankton. American Naturalist 95, 137–145.
Irigoien, X., Huisman, J., Harris, R.P., 2004. Global biodiversity patterns of marine phytoplankton and zooplankton. Nature 429, 863–867.
Kiorboe, T., Saiz, E., Viitasalo, M., 1996. Prey switching behaviour in the planktonic copepod *Acartia tonsa*. Marine Ecology-Progress Series 143, 65–75.
Lima, I.D., Doney, S.C., 2004. A three-dimensional, multinutrient, and size-structured ecosystem model for the North Atlantic. Global Biogeochemical Cycles, 18.
Litchman, E., Klausmeier, C.A., 2001. Competition of phytoplankton under fluctuating light. American Naturalist 157, 170–187.
Litchman, E., Klausmeier, C.A., Schofield, O.M., Falkowski, P.G., 2007. The role of functional traits and trade-offs in structuring phytoplankton communities: scaling from cellular to ecosystem level. Ecology Letters 10, 1170–1181.
Longhurst, A.R., 1998. Ecological Geography of the Sea. Academic Press, San Diego, xiii, 398 p., 394 p. of plates.
Margalef, R., 1978. Life-forms of phytoplankton as survival alternatives in an unstable environment. Oceanologica Acta 1, 493–509.
Martin, J.H., Knauer, G.A., Karl, D.M., Broenkow, W.W., 1987. Vertex—carbon cycling in the northeast Pacific. Deep Sea Research Part I-Oceanographic Research Papers 34, 267–285.
Menden-Deuer, S., Lessard, E.J., 2000. Carbon to volume relationships for dinoflagellates, diatoms, and other protist plankton. Limnology and Oceanography 45, 569–579.
Mickelson, M.J, Maske, H., Dugdale, R.C., 1979. Nutrient-determined dominance in multispecies chemostat cultures of diatoms. Limnology and Oceanography 24, 298–315.
Montoya, J.P., Holl, C.M., Zehr, J.P., Hansen, A., Villareal, T.A., Capone, D.G., 2004. High rates of N-2 fixation by unicellular diazotrophs in the oligotrophic Pacific Ocean. Nature 430, 1027–1031.
Morozov, A.Y., 2010. Emergence of Holling type III zooplankton functional response: bringing together field evidence and mathematical modelling. Journal of Theoretical Biology 265, 45–54.
Murdoch, W.W., Nisbet, R.M., McCauley, E., deRoos, A.M., Gurney, W.S.C., 1998. Plankton abundance and dynamics across nutrient levels: tests of hypotheses. Ecology 79, 1339–1356.
Naselli-Flores, L., Padisak, J., Albay, M., 2007. Shape and size in phytoplankton ecology: do they matter? Hydrobiologia 578, 157–161.
Odum, E.P., 1971. Fundamentals of Ecology, vol. xiv. Saunders, Philadelphia, 574 pp.
Peterson, T.D., Crawford, D.W., Harrison, P.J., 2011. Evolution of the phytoplankton assemblage in a long-lived mesoscale eddy in the eastern Gulf of Alaska. Marine Ecology-Progress Series 424, 53–73.
Redfield, A.C., Ketchum, B.H., Richards, F.E., 1963. The influence of organisms on the composition of sea water. In: Hill, M. (Ed.), The Sea, vol. 2. Interscience, New York, pp. 26–77.
Rosenzweig, M.L., 1995. Species Diversity in Space and Time, vol. xx. Cambridge University Press, Cambridge/New York, 436 pp.
Shannon, C.E., Weaver, W., 1949. The Mathematical Theory of Communication, vol. vii. University of Illinois Press, Urbana, 117 pp.
Smetacek, V., 2001. A watery arms race. Nature 411, 745.
Strom, S.L., 2008. Microbial ecology of ocean biogeochemistry: a community perspective. Science 320, 1043–1045.
Saage, A., Vadstein, O., Sommer, U., 2009. Feeding behaviour of adult *Centropages hamatus* (Copepoda, Calanoida): functional response and selective feeding experiments. Journal of Sea Research 62, 16–21.
Tian, R.C.C., 2006. Toward standard parameterizations in marine biological modeling. Ecological Modelling 199, 128.
Tilman, D., 1977. Resource competition between planktonic algae—experimental and theoretical approach. Ecology 58, 338–348.
Tilman, D., Kilham, S.S., Kilham, P., 1982. Phytoplankton community ecology—the role of limiting nutrients. Annual Review of Ecology and Systematics 13, 349–372.
Waide, R.B., Willig, M.R., Steiner, C.F., Mittelbach, G., Gough, L., Dodson, S.I., Juday, G.P., Parmenter, R., 1999. The relationship between productivity and species richness. Annual Review of Ecology and Systematics 30, 257–300.